JOURNAL OF CRITICAL REVIEWS

ISSN- 2394-5125 VOL 5, ISSUE 07, 2018

Cut-out shapes have a significant effect on the dynamic behaviour of composite thin circular plates.

BANTU SAILESH 1, CHINTA SEKHAR 2,
ASSOCIATE PROFESSOR 2, ASSISTANT PROFESSOR 1,
Mail ID: sailesh.bantu04@gmail.com, Mail ID:sekharresonance1975@gmail.com
Dept.: Mechanical
Nagole Institute of Technology and Science,
Kuntloor(V),Hayathnagar(M),Hyderabad,R.R.Dist.-501505.

ABSTRACT

Effect of cut-out form on fundamental frequency and harmonic response is investigated. circular composite plates that are thin and composite, with the boundaries being kept constant. The Finite Element Method is used for this employed ANSYS Workbench 18.2's SHELL181 module. In all, there are nine unique round plates. characterized by a center equilateral triangle, square, pentagon, hexagon, heptagon, octagon, Patterns of normal nonagons, decagons, and circles have been developed to help us grasp the evolution of the how a building vibrates when its opening geometry approaches a circle. Furthermore, a robust circular plate was modelled so that measurements could be taken and compared. Deeper research on the impact of the slit shape requires everything composites of cross-plies and angle-plies have been used in the design of the constructions. The analysis of vibration at no cost has been completed. to determine the underlying tone frequency of every building. This post will discuss the solution to the harmonic response analysis challenge. using a fixed damping ratio and the Mode Superposition Technique. This study's findings have been understood by taking into account the stress, displacement response, and phase changes at a certain frequency. The According to the findings, the fundamental frequency and harmonic response are significantly impacted by the cut-form. outs of the spherical framework irrespective of Fiber orientation.

Keywords:

Harmonic resonant frequency; Cut-out geometry; Discrete element modelling.

INTRODUCTION

Holes in circular plates have found usage in a wide variety of technological applications. The vulnerability of these structures to stresses that might cause failure has prompted much research on their vibrational characteristics. the phenomenon of resonance, which causes structures to collapse. Furthermore, the enormous stress and potential displacement from the intense vibration imposed by such loads might potentially cause damage to these structures. Several evaluations of structural vibration, such as harmonic response analysis (Sivandi-Pour et al., 2020; elebi et al., 2018; albas Sam., 2021), have been conducted (Yu et al., 2017, Jiaqiang et al., 2018, Jived et al., 2018, and Gonenli & Das, 2021). Several studies that are important to this discussion have been briefly covered (Kumar & Sarangi, 2019; Liu et al., 2021; Son et al., 2021). Take into account the following. Zeng et al. (2019) used Finite Element Analysis to examine the vibration response characteristics that demonstrate the movement of a damaged compressor blade. Kral looked on the resonant behaviour of laminated composites and their harmonics (2014). beams subject to various boundary conditions and confinement sequences. Response of a composite beam to a moving object.Which Gawryluk et al. determined to spin at a constant rate (2019). Abed and Majeed (2020) looked at how boundary circumstances affected the harmonic response of cross-ply and angle-ply composites of different materials and thicknesses. even and Aktaş investigated the modal and harmonic responses of carbon Fiber laminate reinforced concrete railway sleepers (2021). An inner-wall surface discontinuity was the focus of Oka and Khalif's (2020) investigation on the dynamic response of composite pipes used to transport fluids. Using the dynamic stiffness method, Zhang et al. (2018) conducted a harmonic analysis of connected plate structures. The dynamic response of a mass-spring supported, three-beam system under a moving load was investigated by Yuling et al. (2020).

CIRCULAR STRUCTURES AND THE FINITE ELEMENT APPROACH

In order to assess the fundamental natural frequency and the harmonic response of the composite thin circular plates shown in Figure 1, the Finite Element Analysis has been used. A structure's equation of motion looks like this:

$$M\ddot{\delta} + C\dot{\delta} + K\delta = F$$

where the mass, damping, and stiffness matrices are denoted by M, C, and K respectively. The vector F is the external force, while the vector is the generalized displacement coordinates. Various textbooks discuss how to evaluate certain matrices and vectors (Petty, 2010). When calculating a structure's basic natural frequency, it is important to assume that no external force is acting on it and that the damping is also zero. The resulting equation of motion is.

$$M\ddot{\delta} + K\delta = 0$$

Reducing Equation (2) into an eigenvalue problem gives

ISSN- 2394-5125 VOL 5, ISSUE 07, 2018

$$(\boldsymbol{K} - \omega_i^2 \boldsymbol{M})\psi_i = 0$$

the itch natural frequency of the examined structure, and the itch mode shape,the external force and the resulting reaction must be harmonic for the structure to exhibit what is known as a "harmonic response." Taking the complicated external force into consideration as

$$F = F_{max} e^{j\mu} e^{j\Omega t}$$

and the displacement response as

$$r = r_{max} e^{j\gamma} e^{j\Omega t}$$

where Ω is the excitation frequency, γ and μ are the phase shifts of the force and response, respectively. Substituting Equation (5) into Equation (1) and reducing it to eigenvalue problem give

$$(\boldsymbol{K} + j\Omega \boldsymbol{C} - \Omega^2 \boldsymbol{M})\psi_i = F$$

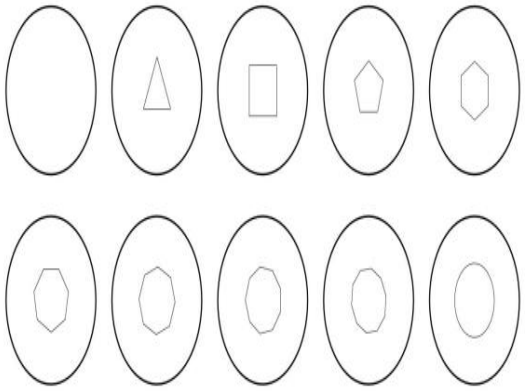

Figure 1. Thin composite circular plates.

Using the results of Equation (3), we can calculate the frequencies needed to solve Equation (5), which yields the structure's response (Petty, 2010). The SHELL181 component of ANSYS Workbench has been taken into account for free vibration analysis as well as harmonic response analysis. For meshing purposes, we have investigated using a triangle element with 6 degrees of freedom. Since the largest achievable mesh size is just 7 mm, the adaptive mesh approach has been used. All buildings were shored up at their outside edges. Each structure's top surface was subjected to a sinusoidal force with a maximum magnitude of 100 N to carry out the harmonic response study. See Figure 2 for an illustration of the mesh structure, harmonic force, and boundary condition used in this case.

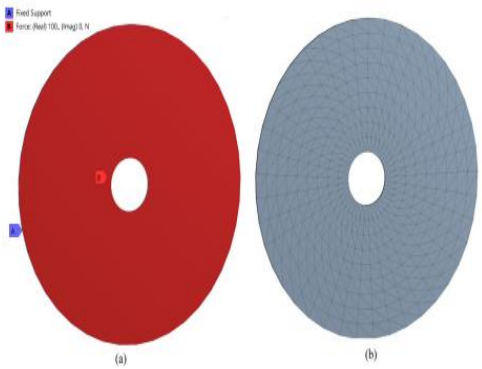

Figure 2. (a) The boundary condition and applied harmonic load; (b) meshed structure.

The harmonic response analysis has been solved using the Mode Superposition Method due to the fact that it is quicker than the Full Method and produces correct findings. The eigenvectors or mode shapes are needed for the Mode Superposition technique, and this may be done using a free vibration analysis. Therefore, free vibration analysis has been done on all structures with the identical boundary conditions in order to examine the influence of cut-out shape on the fundamental frequency and meet the criteria specified above. To make sure the response can be seen, the frequency range was calculated by multiplying the fundamental frequency by 1.5. The damping effect, presented as the material damping coefficient by =0.02 (Kraal, 2014), allows for more precise and reasonable outcomes. We have analysed the frequency-displacement, frequency-phase angle, critical-frequency displacement, and critical-frequency stress graphs.

STATISTICAL CONCLUSIONS

The examined circular structure's geometric features are listed in Table 1. Epoxy carbon composite with a single direction of carbon Fiber has been proposed as the composite material. The following are some characteristics of the material: Where Ex= 121 GPa, Ey= 8.6 GPa, Gx= 4.7 GPa, Gyz= 3.1 GPa, vxy= xz= 0.27, yz= 0.4, where Ex, Ey, andEz are the modulus of elasticity with respect to the x-, y-, and z-axes, Gx, Gxz, and Gyz are the shear modulus with regard to the.

Table 1. Geometrical properties of considered structures

ISSN- 2394-5125 VOL 5, ISSUE 07, 2018

Property	Symbol	Value
Circular Plate Diameter	d	300 mm
Circular Plate Thickness	t	3 mm
Cut-Out Area	A_c	1963.5 mm^2

By rounding off the cut-out's edges, it was possible to study its impact on the design. By increasing the number of edges from 3 to infinity, the roughness has been significantly reduced (equilateral triangle to circular). With a 50 mm diameter circular cut-out in mind, we were able to calculate the constant cut-out area. This fixed cut-out portion informed the design of all subsequent openings. Cut-outs vary in area (1963.5 mm2) but have varying lengths of edges. The findings have been compared to those found by Sun et al. (2021) to ensure their accuracy. Composite circular plates with square cut-outs of 100 x 100 mm, 200 x 200 mm, and 300 x 300 mm, each having a diameter of 1000 mm and a thickness of 10 mm, and five layers (00 /300 /450 /600 /900) have been examined for this purpose. The material characteristics are detailed in the associated research (Sun et al., 2021). Results from a comparison study using the nondimensional fundamental frequency, +, = 512-dd, are shown in Table 2. (1 /" "/)/EE/tt0, where is the natural frequency, d is the diameter, E1 is the modulus of elasticity of the composite material with respect to the x-axis, and v12 and 21 are the Poisson's ratios (Sun et al., 2021).

Table 2. Nondimensional comparative analysis results (Cs: cut-out size).

Frequency Mode	Cs=100x100 mm		Cs=200x200 mm		Cs=300x300 mm	
	Present Study (ANSYS)	Sun et al. (2021)	Present Study (ANSYS)	Sun et al. (2021)	Present Study (ANSYS)	Sun et al. (2021)
1	13.8769	14.0171	14.6178	14.9673	16.8574	17.2956
2	27.7943	27.7297	26.3399	26.9835	25.5896	26.3601
3	28.4032	28.3875	26.8451	27.5683	25.9336	26.8029
4	44.0324	44.3372	41.6928	42.6750	40.7880	41.8831
5	45.4892	45.1408	42.7731	43.4541	41.3441	42.4390

Table 2 shows that the considered method's free vibration findings are quite consistent with those of Sun et al (2021). The cut-out forms of thin cross ply and angle-ply circular plates are shown in Table 3, and their corresponding fundamental frequencies are listed in Table 4.

Table 3. Nondimensional fundamental frequencies of cross-ply circular plates.

Frequency (λ_{nd})	No Cut-Out	Equilateral Triangular Cut-Out	Square Cut-Out	Regular Pentagon Cut-Out	Regular Hexagon Cut-Out
1	106.6451	136.1910	150.6220	141.9210	150.1756
Frequency (λ_{nd})	**Regular Heptagon Cut-Out**	**Regular Octagon Cut-Out**	**Regular Nonagon Cut-Out**	**Regular Decagon Cut-Out**	**Circular Cut-Out**
1	155.9056	146.6802	144.7556	161.6618	155.3028

Table 4. Nondimensional fundamental frequencies of angle-ply circular.

Frequency (λ_{nd})	No Cut-Out	Equilateral Triangular Cut-Out	Square Cut-Out	Regular Pentagon Cut-Out	Regular Hexagon Cut-Out
1	106.3524	135.9156	150.6219	141.7298	150.1234
Frequency (λ_{nd})	**Regular Heptagon Cut-Out**	**Regular Octagon Cut-Out**	**Regular Nonagon Cut-Out**	**Regular Decagon Cut-Out**	**Circular Cut-Out**
1	155.6622	146.5787	144.7093	161.4241	155.2158

It can be shown in Tables 4 and 5 that the fundamental natural frequencies of the circular plates with cut-outs are greater than those of the same plates without cut-outs. The frequency value seems to be on the rise, but it really drops when more regular shapes (such as pentagons, octagons, and nonagons) are included into the building. The fundamental frequency of the circular structure with a circular cut out is much greater than that with an equilateral triangular cut out, as can be shown by comparing the two cut-outs with different numbers of edges. It is found that the fundamental frequencies of the structure with the angle-ply Fiber orientation are somewhat lower (about 1Hz) than those of the structure with the cross-ply Fiber sequence. The maximum stress and

ISSN- 2394-5125 VOL 5, ISSUE 07, 2018

maximum displacement values, as well as the phase shift, are shown in Table 5, and the harmonic response analysis findings are shown in Table 6. The frequency response and frequency phase diagram of the cross-ply circular plate with a center regular decagon cut - out are shown in Figure 3. Take note that the frequency response and frequency phase of all other structures is same. Variations in frequency, responsiveness, and phase are the sole distinguishing characteristics. Figure 3(a) shows that the strongest reactions occurred at the fundamental frequency of each structure. For all spherical structures, the phase shift is also present at the fundamental frequency.

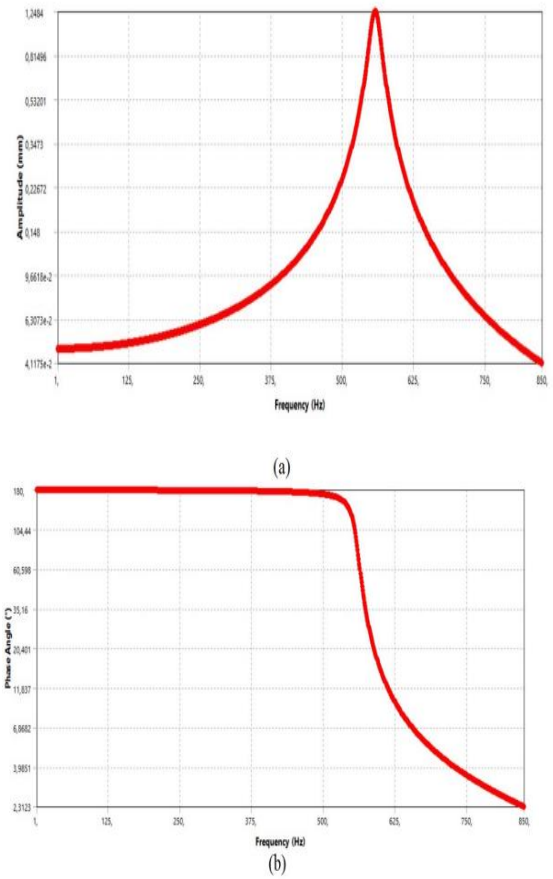

Figure 3. (a) The frequency-displacement response and (b) frequency-phase diagram of cross-ply circular plate having central regular decagon cut-out.

Table 5. Harmonic response analysis results of cross-ply circular plates.

Parameter	No Cut-Out	Equilateral Triangular Cut-Out	Square Cut-Out	Regular Pentagon Cut-Out	Regular Hexagon Cut-Out
Phase Shift (^{0})	89.464	95.296	93.633	93.725	90.644
Maximum Stress (MPa)	126.560	173.690	83.656	113.260	95.264
Maximum Displacement (mm)	2.5323	1.7661	1.4321	1.6046	1.4527
Parameter	**Regular Heptagon Cut-Out**	**Regular Octagon Cut-Out**	**Regular Nonagon Cut-Out**	**Regular Decagon Cut-Out**	**Circular Cut-Out**
Phase Shift (^{0})	89.39	90.338	92.387	93.834	88.946
Maximum Stress (MPa)	84.344	93.996	94.369	74.814	81.338
Maximum Displacement (mm)	1.3339	1.4988	1.5501	1.2476	1.3455

Table 6. Harmonic response analysis results of angle-ply circular plates.

Parameter	No Cut-Out	Equilateral Triangular Cut-Out	Square Cut-Out	Regular Pentagon Cut-Out	Regular Hexagon Cut-Out
Phase Shift (^{0})	89.511	89.64	93.73	90.008	89.789
Maximum Stress (MPa)	129.550	175.810	116.430	112.710	99.445
Maximum Displacement (mm)	2.5517	1.7805	1.4391	1.6079	1.4481
Parameter	**Regular Heptagon Cut-Out**	**Regular Octagon Cut-Out**	**Regular Nonagon Cut-Out**	**Regular Decagon Cut-Out**	**Circular Cut-Out**
Phase Shift (^{0})	90.35	88.481	91.606	89.759	92.84
Maximum Stress (MPa)	80.051	85.487	95.635	76.639	82.252
Maximum Displacement (mm)	1.3405	1.5032	1.5526	1.2545	1.3541

Tables 5 and 6 shows that the phase shift has been slightly affected by Fiber angles, with the maximum value evaluated for the cross-ply circular structure with a triangular cut-out (95.2960) and the minimum value obtained for the angle-ply circular structure with a regular octagon cut-out (88.4810). The angle-ply construction with a central equilateral triangle cut-out (175.810 MPa) was found to have the highest stress value, while the cross-ply structure with a regular decagon cut-out was found to have the lowest stress value (74.814 MPa). The only significant variation in stress values across Fiber orientations is shown for the square cut-out structure, where the stress value is 83.656 MPa for the cross-ply orientation and 116.43 MPa for the angle-ply sequence. As a result of the shift in Fiber orientation, other structures

ISSN- 2394-5125 VOL 5, ISSUE 07, 2018

have also been impacted. While noticeable, these shifts are negligible (up to 5MPa) in comparison to the square cut-out. Based on the measured displacements, we can conclude that the angle-ply structure without a cut-out experienced the greatest amount of movement, measuring in at 2.5517 mm, while the cross-ply structure with a regular decagon cut-out was evaluated as having the least amount of movement, measuring in at 1.2476 mm. Since the greatest displacement difference of 0.0194 mm has been found for the structure with no cut-outs, the effect of Fiber orientation on the displacement of the structure is minimal. So, it's safe to say that the cut-form outshave a major impact on the structure's sensitivity to displacement. When analysed in terms of phase shift values, all configurations indicate that there is no hard and fast relationship between the number of cut-out edges and the fibber's orientation. As the number of cut edges rises, there is a corresponding increase in stress levels. For all sequences of stacking, however, the stress levels tend to decrease as the number of edges of the cut-outs rises, in contrast to the phase shifts. In both Fiber orientations, the displacement reaction decreases as the edge number of cut-outs increases, reflecting the stress trend. The findings of the harmonic response analysis reveal a consistent pattern in the stress distribution. Figure presents the stress patterns of cross-ply and angle-ply circular plates. 4.

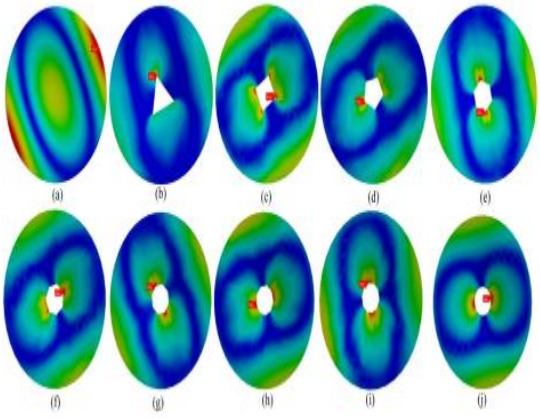

Figure 4. Harmonic stress distributions in circular cross-ply and angle-ply systems. Figure 4 shows that the highest stress shifts to the area surrounding the cut-out from the periphery of the structure when a central cut-out of any form is present. When there is a lot of variety in the form of the cut-outs, the tension is distributed in a lot of different ways. The blue area has the lowest stress (about 0 MPa), followed by the green, yellow, and red areas, which have the greatest. Figure 4 shows that when the number of edges of the cut-outs grows, the area of light green and green areas gets smoother. Consequently, the circular cut-out has been shown to have the smoothest distribution. However, the cut-out form also modifies the stress distribution in the periphery and core of circular constructions that have openings. Tables 5 and 6 shows that the stress values for the constructions with an equilateral triangle cut-out are the greatest, but that there is a sharp drop down when the stress approaches zero in the blue zone. No of the form of the cut-out, the largest tension is always found towards the corners or along the edge. The displacement values of cross-ply and angle-ply constructions vary, but the displacement zones are the same. Figure 5 displays displacement maps for both cross-ply and angle-ply circular plates.

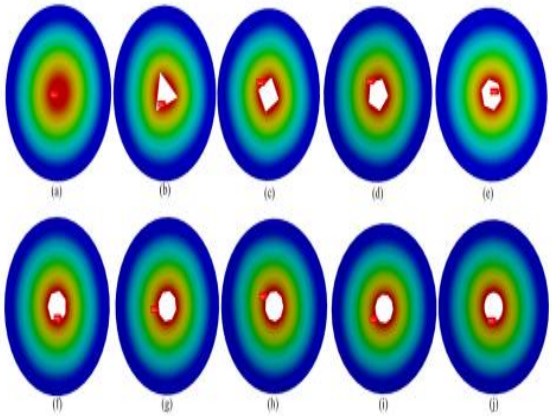

Figure 5. Plots of displacement for circular cross-ply and angle-ply constructions under harmonic stress.

Displacement reactions of all structures function similarly, as shown by the plots in Figure 5, independent of the presence or form of the cut-out. On top of that, the forms of the initial modes of all structures are identical to the displacement plots of all structures.

CONCLUSION

The basic natural frequency and harmonic response of thin composite circular constructions with various cut-out shapes have been studied in this research. The following conclusions are reached from the numerical results:

Regardless of the Fiber orientation, the fundamental frequency values tend to rise as the form of the cut-out approaches a perfect circle. No of the fibber's polarity, the phase shift is little impacted by the cut-out's geometry.

ISSN- 2394-5125 VOL 5, ISSUE 07, 2018

• As the form of the opening approaches a circle, there is a declining tendency in the displacement reactions. We find that the building with an equilateral triangle taken out has the most displacement, whereas the one with a regular decagon cut out has the least.

• The presence of cut-outs, the shape of cut-outs, and the orientation of fibers had no effect on the distribution of the displacement reaction. Since the highest response occurred at the fundamental frequency, the graphs of the displacement response are identical to those of the form of the fundamental mode. The fibber's displacement response is mostly unaffected by its orientation.

• As the form of the opening approaches a circle, a decreasing stress value trend is seen. The stress is found to be greatest for the equilateral triangle cut-out and the least for the conventional decagon cut-out. Maximum stress values are only marginally affected by Fiber orientation, and even then, only in the square cut-out structure.

• The geometry of the cut-out has had a significant impact on the stress distribution. As the shape of the opening becomes closer and closer to a perfect circle, the stress distribution becomes more even and uniform. As the number of cut-out edges grows, the stress areas where stress values range from zero to maximum become more distinct.

• The highest stress is transferred from the edge to the middle of the structure as a result of the cut-out's presence.

REFERENCES

[1] Jived, S., Viswanathan, K. K., Nurul Izyan, M. D., Aziz, Z. A., & Lee, J. H. 2018. Free vibration of cross-ply laminated plates based on higher-order shear deformation theory. Steel and Composite Structures. 26 (4): 473-484.

[2] Gonenli, C., & Das, O. 2021. Effect of crack location on buckling and dynamic stability in plate frame structures. Journal of the Brazilian Society of Mechanical Sciences and Engineering. 43: 311.

[3] Yui Y., Zhang, S., Li, H., Wang, X., & Tiang, Y. 2017. Modal and harmonic response analysis of key components of ditch device based on ANSYS. Procedia Engineering, 174: 956-964.

[4] Jiaqiang, E., Liu, G., Liu, T., Zhang, Z., Zuo, H., Hu, W., & Wei, K. 2019. Harmonic response analysis of a large dish solar thermal power generation system with wind-induced vibration. Solar Energy. 181: 116-129.

[5] Kumar, M., & Sarangi, S. K. 2020. Harmonic response of carbon nanotube reinforced functionally graded beam by finite element method. Materials Today: Proceedings. 44(6): 4531-4536.

[6] Zeng J., Chen, K., Ma, H., Duan, T., & Wen, B. 2019. Vibration response analysis of a cracked rotating compressor blade during run-up process. Mechanical Systems and Signal Processing. 118: 568-583.

[7] Kıral, Z. 2014. Harmonic response analysis of symmetric laminated composite beams with different boundary conditions. Science and Engineering of Composite Materials. 21(4): 568-583.

[8] Gawryluk, J., Mitura, A., & Teter, A. 2019. Dynamic response of a composite beam rotating at constant speed caused by harmonic excitation with MFC actuator. Composite Structures. 210: 657-662.

[9] Abed, Z. A. K., & Majeed, W. I. 2020. Effect of boundary conditions on harmonic response of laminated plates. Composite Materials and Engineering. 2(2): 125-140.

[10] Çeçen, F., & Aktaş, B. 2021. Modal and harmonic response analysis of new CFRP laminate reinforced concrete railway sleepers. Engineering Failure Analysis. 127: 105471.

[11] Oke, W. A., & Khulief, Y. A. 2020. Dynamic response analysis of composite pipes conveying fluid in the presence of internal wall thinning. Journal of Engineering Mechanics. 146(10): 04020118.

[12] Zhang, C., Jin, G., Ye, T., & Zhang, Y. 2018. Harmonic response analysis of coupled plate structures using the dynamic stiffness method. Thin-Walled Structures. 127: 402-415.

[13] Yulin, F., Lizhong, J., & Zhou, W. 2020. Dynamic response of a three-beam system with intermediate elastic connections under a moving load/mass-spring. Earthquake Engineering and Vibration. 19(2): 377-395.

[14] ANSYS@ Workbench, Release 18.2. Petyt, M. 2010. Introduction to Finite Element Analysis. Cambridge: Cambridge University Press. Sun, X., Zhang, P., Qiao, H, & Lin, K. 2021. High order free vibration analysis of elastic plates with multiple cutouts. Archive of Applied Mechanics. 91: 1837-1858.

[15] Albassam, B. 2021. Vibration control of a linear flexible beam structure excited by multiple harmonics. Journal of Engineering Research. 9(4B): 410-427.

[16] Çelebi, K., Yarımpabuç, D., & Baran, T. 2018. Forced vibration analysis of inhomogeneous rods with nonuniform cross-section. Journal of Engineering Research. 6(3): 189-202.

[17] Sivandi-Pour, A., Farsangi, E. N., Takewaki, I. 2020. Estimation of Vibration Frequency of Structural Floors Using Combined Artificial Intelligence and Finite Element Simulation. Journal of Engineering Research. 8(3): 1-16.